Biosensors and Bioelectronics 86 (2016) 75–82

Contents lists available at ScienceDirect

Biosensors and Bioelectronics

journal homepage: www.elsevier.com/locate/bios

An electrochemical biosensor for double-stranded Wnt7B gene detection based on enzymatic isothermal amplification

Junlong Li [a], Zhongping Chen [b], Yu Xiang [c], Lili Zhou [a], Ting Wang [a], Zhang Zhang [a], Kexin Sun [a], Dan Yin [a], Yi Li [a], Guoming Xie [a,*]

[a] Key Laboratory of Laboratory Medical Diagnostics, Ministry of Education, Department of Laboratory Medicine, Chongqing Medical University, Chongqing 400016, PR China
[b] Department of Clinical Laboratory, Chongqing Municipal Jiulongpo District People's Hospital, Chongqing 400050, PR China
[c] Department of Chemistry, Tsinghua University, Beijing 100084, PR China

ARTICLE INFO

Article history:
Received 28 March 2016
Received in revised form
10 June 2016
Accepted 11 June 2016
Available online 14 June 2016

Keywords:
Electrochemical biosensor
Double-stranded DNA detection
Isothermal amplification
Wnt7B gene

ABSTRACT

Wnt7B gene plays an important role in the development and progression of breast cancer, gastric cancer, esophageal cancer and pancreatic cancer. While, the natural state of DNA is double stranded, which makes it difficult to be directly detected. Here, we develop an electrochemical biosensor method for Wnt7B gene detection without the need to denature the target. This method firstly used nicking enzyme for exploiting in the double-stranded DNA (dsDNA). Then, long single-stranded DNA (ssDNA) was generated from the cutting site through polymerase extension reaction. Whereafter, the long ssDNA triggered a hairpin self-assembly recycling reaction, which gave rise to another isothermal amplification reaction. Last, short ssDNA was formed after the this amplification process, which could hybridize with the capture probe immobilized on Au electrode and result in signal variation. This method showed excellent analytical performance for dsDNA, of which the linear range was 2 fM to 500 pM and the detection limit was 1.6 fM (S/N=3). It also showed an good results when applied to the real sample of Wnt7B gene detection.

1. Introduction

Wnt7B gene (NCBI reference sequence: NC_000022.11), which consists of structurally related genes that encode secreted signaling proteins (Almario and Karakas, 2015). The proteins encode by this gene have been implicated in oncogenesis and several developmental processes, including regulation of cell fate and patterning during embryogenesis. This gene may play important roles in the development and progression of breast cancer, gastric cancer, esophageal cancer and pancreatic cancer. (http://www.ncbi.nlm.nih.gov/gene?Db=gene&Cmd=ShowDetailView&TermToSearch=7477, last accessed 15 March 2016).

In recent years, there are many reports about nucleic acid detection for its huge potential in clinical disease diagnosis (Xuan and Hsing, 2014; Cai et al., 2014; Ghindilis et al., 2015; Hun et al., 2015; Li et al., 2015; Xu et al., 2015; Zhu et al., 2015b). Lots of ultrasensitive nucleic acid testing methods have been proposed. While, they just have been used to synthesize short single-stranded DNA (ssDNA) to detect. The natural state of DNA in real samples is long and double strand, which makes it not easy to be accurately detected. Moreover, the content of target in real samples is low. To solve this difficulty, some detection methods based on polymerase chain reaction (PCR) derived techniques are developed, such as asymmetric PCR (Campuzano et al., 2011; Chen et al., 2013), magnetic separation (Stevenson et al., 2008; Ma et al., 2012), size separation on denaturing urea polyacrylamide gel electrophoresis (Marimuthu et al., 2012; Liang et al., 2015) and toehold-mediated DNA strand displacement (Khodakov et al., 2013). Although these methods can generate ssDNA or single-stranded toehold, there are also different weaknesses to limit their use in bioanalysis. Such as, the products of asymmetric PCR are still very long; Both DNA biotin-streptavidin separation and size separation on denaturing urea polyacrylamide gel electrophoresis need complex experimental procedures. Toehold-mediated DNA strand displacement is subjected to the difficulty of long-chain probe synthesis. Furthermore, all of these methods need electrically powered thermal cycling equipment for repeated heating and cooling processes (Yang and Rothman, 2004; Giljohann and Mirkin, 2009).

To date, some isothermal nucleic acid amplification approaches have been developed for DNA detection. For example, rolling circle

* Corresponding author.
E-mail addresses: guomingxie@cqmu.edu.cn, xiegm059@foxmail.com (G. Xie).

http://dx.doi.org/10.1016/j.bios.2016.06.031
0956-5663/

amplification (RCA) (Schweitzer et al., 2002; Ali et al., 2014), loop-mediated isothermal amplification (LAMP) (Notomi et al., 2000; Wong et al., 2014) and helicase-dependent amplification (HDA) (Vincent et al., 2004; Barreda-Garcia et al., 2015). There are some advantages of these approaches over PCR derived techniques in that they no need repeat thermal cycling processes. While, these amplification methods need to convert double-stranded DNA (dsDNA) to single-stranded template at first, resulting in complex steps of experiment. What's more, these amplification products are dsDNA or long-chain DNA, which can not be directly detected by the biosensor. Exponential amplification reaction (EXPAR), as an amplification technique that combines polymerase strand extension and single-strand nicking, has high amplification efficiency and rapid amplification kinetics (Van Ness et al., 2003). This method has the distinct advantages that it directly gets ssDNA from double-stranded target. Therefore, EXPAR has huge potential for dsDNA detection.

Herein, for the first time, we reported a novel, practical isothermal amplification method for double-stranded oncogene detection. Firstly, long ssDNA obtain from dsDNA samples through the combined action of nicking enzyme and polymerase (Jia et al., 2010; Qian et al., 2012; Nie et al., 2015; Shi et al., 2016). Then, hairpin self-assembly trigger recycling happen in the presence of ssDNA (Yin et al., 2008; Wu et al., 2015; Zang et al., 2016). In this catalytic process, the long ssDNA acts on kinetically trapped substrates via exposed toehold and strand exchange reaction with hairpin structure, refolding the substrate and allowing them to interact with one another (Jung and Ellington, 2014). On account of the hairpin structure is ingeniously designed according to the input ssDNA, only well-matched long ssDNA could trigger the hairpin self-assembly circular reaction, which could insure the specificity of the reaction (Ma et al., 2015). The new dsDNA generated in the reaction go ahead another enzyme amplification reaction. Short ssDNA appeared at last, which can be detected conveniently and easily. Meanwhile, since the electrochemical DNA (E-DNA) sensor was first developed by Fan et al. for nucleic acid detection (Fan et al., 2003), it had received substantial attention (Liu et al., 2008; Lin et al., 2014; Wang et al., 2015; Wang et al., 2016). In this method, short ssDNA binding induced conformational changes of the redox tag labeled stem-loop capture probe (Cp), which can be monitored by detecting the distance-dependent electron transfer between the attached signal molecules and the electrode. This E-DNA sensor does not need target labeling, which can be used to detect DNA rapidly and simply.

2. Experimental

2.1. Reagents and materials

All oligonucleotide sequences were synthesized and purchased from Sangon Biotechnology Co. (Shanghai, China), and the oligonucleotide sequences were provided in Table 1. 6-Mercapto-1-hexanol (MCH) was obtained from Sigma-Aldrich (St. Louis, USA). Bst 2.0 WarmStart™ DNA polymerase, Nt. BstNBI nicking enzyme and NEBuffer 3.1 (10 ×) were purchased from New England Biolabs, Inc. (Beverly, MA, USA). Goodview nucleic™ acid stain (HGV-II) was purchased from SBS Genetech Co., Ltd. (Beijing, China). Deoxynucleotide triphosphates (dNTPs) were obtained from Thermo Fisher Scientific (Massachusetts, USA). Premix Taq™ (TaKaRa Taq™ Version 2.0 plus dye), 20 bp DNA Ladder, DL 500 DNA marker and loading buffer (6 ×) were purchased from TaKaRa Biotechnology Co. Ltd. (Dalian, China). Agarose G-10 was obtained from Biowest. TIANamp Genomic DNA Kit was purchased from TIANGEN Biotech Co. Ltd. (Beijing, China). Cell lines of MDA-MB-231 and 293T were obtained from Shanghai Institute for Biological Sciences, Chinese Academy of Science. Dulbecco modified eagle medium (DMEM) and fetal bovine serum were obtained from Gibco (New York, USA). Buffer for electrochemical impedance spectroscopy (EIS)**:** 0.1 M PBS, 5 mM $[Fe(CN)_6]^{3-/4-}$ and 0.1 M KCl (pH 7.0). Buffer for cyclic voltammetry (CV) and Square Wave Voltammetry (SWV)**:** 20 mM Tris–HCl, 140 mM NaCl, and 5 mM $MgCl_2$ (pH 7.4). Ultrapure water (Milli-Q18.2 MΩ, Millipore System Inc.) was used for all the experiments.

2.2. Instrumentations

All electrochemical measurements were performed on a CHI660D electrochemical workstation (Shanghai CH Instruments Co., China). A conventional three component electrochemical cell

Table 1
Sequences of the oigonucleotides[a].

Oligonucleotides	Sequence (from 5′ to 3′)
Capture probe (Cp)	SH-$(CH2)_6$-GCCTGCGTATACTTCAAAAGCCCTTCACACGCAGGC-MB
H1	ATACTTCAAAAGCCCTTCACTCCTGACTCTGAATGCCCCACCCTCAGTCCGATAAGCGAGGGTGGGGCATTCACGGTGGCC
H2	AGTCCGATAAGCTGAATGCCCCACCCTCGCTTATCGGACTGAGGGT
S1	TGGACGCTCTGAGTCTCCGGGCCACCGTGAATGCCCCACCCTCAGCCTGGCCCCATCCC
S2	GGGATGGGGCCAGGCTGAGGGTGGGGCATTCACGGTGGCCCGGAG ACTCAGAGCGTCCA
S3	TGGACGCTCTG**C**GTCTCCGGGCCACCGTGAATGCCCCACCCTCAGC CTGGCCCCATCCC
S4	GGGATGGGGCCAGGCTGAGGGTGGGGCATTCACGGTGGCCCGGAGACGCAGAGCGTCCA
Input	GGCCACCGTGAATGCCCCACCCTCAGCCTGGCCCCATCCC
Single-base mismatch input	GGCCACC**C**TGAATGCCCCACCCTCAGCCTGGCCCCATCCC
Two-base mismatch input	GGCCAC**GC**TGAATGCCCCACCCTCAGCCTGGCCCCATCCC
Random DNA	GGCCCGGCAGCCTCTGCAAGGAACCTGGTTAACTTATGTT
S5	ATAGACTCTAGC
S6	CCCCCACAATCTATTC-Dabcyl
S7	FAM-GAATAGATTGTGGGGGTCCTCAGCTAGAGTCTAT
Forward primer	GAAGCAGGGCTACTACAACCA
Reverse primer	CGGCCTCATTGTTATGCAGGT

[a] The underlined letters of H1 represent its cutting enzyme recognition domain. The bold letters in single-base mismatch input and two-base mismatch input mean false priming site, respectively. The underlined letters in S1 mean the cutting enzyme recognition domain. The bold letter in S3 means one base variation in cutting enzyme recognition domain.

was employed in all electrochemical measurements, with a modified Au electrode as the working electrode, a KCl-saturated Ag/AgCl electrode as the reference electrode and a Pt wire as the auxiliary electrode. EIS and CV measurements were used to monitor the interface properties of the modified electrode. Fluorescence signals were recorded using a Cary Eclipse Fluorescence spectrophotometer (Agilent, California). Parameters: Scan time, 10 min; Scanning intervals, 2 min; Integration time, 6 s; Excitation slit, 5 nm; Emission slit, 10 nm; Excitation wavelength, 490 nm; Emission wavelength, 520 nm. Inverted microscope (TE, 2000-V, Nikon, Japan) was used to observe cells. UV–visible absorption spectroscopy (NANO-DROP1000 Spectrophotometer, Thermo, USA) was used to investigate the concentration of cell extracts. Electrophoresis apparatus (DYY-6C, LIUYI, China) was used in all gel electrophoresis experiments. Gel images were recorded on an imaging system (Bio-Rad Laboratories, USA). PCR was finished by T100™ thermal cycler (Bio-Rad Laboratories, USA).

2.3. Isothermal amplification system

The system in 10 μL contained 1.0×10^{-7} M H1, 1.2×10^{-7} M H2, 4×10^{-4} M dNTPs, 2 U Bst 2.0 WarmStart™ DNA polymerase, 4 U Nt.BstNBI nicking enzyme, 1 × NEBuffer 3.1 (100 mM NaCl, 50 mM Tris–HCl, 10 mM $MgCl_2$, 100 μg/mL BSA, pH 7.9, T 25 °C). The reaction was initiated by adding different concentrations of target and incubated at 55 °C for 40 min

2.4. Fabrication of biosensor and electrochemical detection

The Au electrode (3 mm diameter) was polished with alumina powder of 0.3 and 0.05 μm for 10 min, then sequentially sonicated each in ultrapure water, ethanol, and ultrapure water for 10 min, respectively. Whereafter, it was infused in freshly prepared piranha solution (3:1 concentrated 98% H_2SO_4: 30% H_2O_2. *Caution: piranha solution reacts violently with organic compounds, and it should not be stored in closed containers*) for 10 min and washed through ultrapure water. Then, 10 μL of 1 μM Cp was dropped on to the surface of Au electrode and incubated for 8 h at RT, followed by a thorough washing with washing buffer. Subsequently, the electrode was immersed into 1 mM MCH for 1 h to block the remaining bare region. The Cp was anchored via a Au–S bond between the Au surface and the 5′-hexanethiol tethers (C6SH), whose length matched that of MCH, which was used to passivate the Au surface.

10 μL of isothermal amplification solution was dropped on to the surface of biosensor and incubated for 2 h at RT, followed by a thorough washing with washing buffer. SWV were carried out from −0.6 to 0 V with amplitude of 25 mV and frequency of 25 Hz in Tris–HCl (pH 7.4, 20 mM). All measurements were obtained at room temperature (RT, 25 ± 2.0 °C).

2.5. Gel electrophoresis

Electrophoresis analysis in Fig. 1A, B and Fig. 5A was carried out on 3.5%, 3.5% and 2% agarose gels, respectively. The nucleic acid dye was HGV-II nucleic acid dye staining. The agarose gels in Fig. 1A and B were ran at 80 V for 40 min in 0.5 × tris-borate-EDTA buffer (TBE, pH 8.1) at RT. The agarose gels in Fig. 5A were ran at 120 V for 45 min. Electrophoresis apparatus was used for the electrophoresis experiments. At last, the gels were photographed by Bio-RAD digital imaging system.

2.6. Cell culture and DNA extraction

The MDA-MB-231 cells and 293T cells (Fig. S1) were routinely cultured in full DMEM (41965062) containing 10% fetal bovine serum (100099-133) at 37 °C incubator containing 5% CO_2. Cells were cultured in 2 mL DMEM + 10% FBS per well in 6-well plates and grown to approximate 80%. The density and morphology of cells were observed by using inverted microscope. DNA was isolated from MDA-MB-231 cells and 293T cells using TIANamp Genomic DNA Kit (DP304) according to the manufacture's protocol, respectively. DNA concentrations obtained from 3 plates 231 cells were measured by UV–visible absorption spectroscopy.

2.7. PCR

PCR was performed in a final volume of 10 μL containing 1.1 μL of cDNA, 0.22 μL of 100 μM each primer, 5 μL of Premix Taq and 3.46 μL of ddH_2O. DNA was initially denatured at 94 °C for 5 min, followed by 34 cycles of 94 °C for 30 s (denaturation), 59 °C for 30 s (annealing), 72 °C for 20 s (extension), and final 5 min extension.

2.8. Reproducibility and stability experiments

The reproducibility of this method was assessed by testing the reaction products in the presence of 0.01 pM, 1 pM, and 100 pM double-stranded targets (S1/S2). Target at the same concentration levels were tested 6 times. Firstly, under the optimized conditions, targets were reacting for 40 min at 55 °C. Then, 10 μL of reaction solution was dropped on to the surface of biosensor and incubated for 2 h at RT. At last, the biosensor were detected by electrochemical workstation.

The stability of the biosensor was tested by storing the biosensor of MCH/Cp/Au at 4 °C. At first, a new biosensor was fabricated and detected. Then, the biosensor was stored at 4 °C for two weeks. After that, this biosensor was detected at the same condition.

3. Results and discussion

3.1. Principle of this method

The principle of this method was illustrated in Scheme 1. The dsDNA was extracted from cells at first. Then, the restriction enzyme cutting site in dsDNA was recognized and nicked by nicking enzyme (Nt. BstNBI, 5′-GAGTCNNNN$^{\downarrow}$N-3′). The nicked restriction enzyme cutting site then initiated polymerization reaction and strand displacement reaction cycle to produce long ssDNA continually, which was used as “input” in this system. Hairpin H1 and H2 (shown in Fig. S2) contained an occluding complementary regions within intramolecular hairpin secondary structures, respectively. When challenged with input, H1 partly hybridized with input and underwent a conformational change to form a input/H1 complex. After that, the unfolded domain of H1 served as a “toehold” to initiate interaction with H2, leading to a branch migration process. The branch migration process then displaced input strand and formed a H1/H2 complex. The released input was free to interact with one another H1. Meanwhile, another polymerization reaction can be initiated by the hybridization of H1 and H2, in which H2 acted as primer and the 3′ terminal of H2 extended along the H1 template, then form a new restriction enzyme cutting site. Whereafter, one more amplification reaction, which contained nicking process, polymerization reaction, and displacement reaction, was initiated upon the nicking enzyme and polymerase. Finally, short ssDNA named “output” was generated in the series of reaction. The output could hybridize with the loop region of Cp, which was labeled with 3′-methylene blue (MB) and immobilized on the Au electrode surface, and force its stem open. With the conformational change of Cp, the MB molecule of Cp

went away from the electrode surface, which led to a reduction of the electrochemical signal. Eventually, a significant suppression of electrochemical signal through conformational change was obtained for dsDNA detection by a series of isothermal amplification reaction. Furthermore, the ssDNA input extraction and multiple signal recycling amplification steps all took place in solution, which could reduce interfacial effect and improve reaction efficiency (Xue et al., 2011).

3.2. Characterization

3.2.1. Gel electrophoresis characterization of the process of isothermal amplification reaction

Two dsDNA (S1/S2, S3/S4) were used to confirm the process of isothermal amplification reaction. As shown in Fig. 1A, S1/S2 was the double-stranded target owned enzyme cutting site. Simultaneously, S3/S4 acted as negative control dsDNA without enzyme cutting site. In the presence of cutting site for the nicking enzyme, the amplification reaction could be performed. S1/S2 amplification products without added cutting enzyme as blank group (lane 1). The amplification products of control S3/S4 were presented in lane 2, which were no obvious change compared with blank group. However, the amplification products of S1/S2 were appeared complicated bands (lane 3), because different complex structures were produced with the polymerization and displacement reactions continually proceed. Therefore, these observations showed the isothermal amplification process take place in this reaction. Meanwhile, the performance of polymerase is very well at 55 °C, the results shown in Fig. S3.

3.2.2. Gel electrophoresis characterization of hairpin self-assembly triggered recycling reaction

The process of hairpin self-assembly triggered recycling was verified using input strand and random strand with agarose gel electrophoresis (Fig. 1B). In the absence of input ssDNA, the cross reaction between H1 (lane 2) and H2 (lane 3) was effectively blocked (lane 4). While, after mixing with input strand, hybridization of H1 and H2 was initiated, resulting in a stable H1/H2 duplex (lane 6). In addition, the presence of random DNA could not trigger the cross interaction between H1 and H2 (lane 8). A new band of lower mobility appeared after input DNA mixed with H1 (lane 5). While, it did not turn up when random DNA mixed with H1 (lane 7). The electrophoresis results suggested that right input DNA could open hairpin H1 and trigger hairpin self-assembly triggered recycling. The final concentration of Input, Random, H1 and H2 were all set as 1 μM, all the reaction proceed at 55 °C.

3.2.3. Electrochemical characterization of the biosensor

Each step of the working electrode preparation were shown in Fig. 2A. CV was used to characterize the conformational change of the Cp on the Au electrode surface. As shown in Fig. 2B, no redox peak was detected on bare electrode, for no redox indicator was introduced to the Au electrode surface (curve 1). A couple of strong redox peaks were observed (curve 2), which indicated the MB-modified capture probes were immobilized on the surface of Au electrode. The redox peaks had not changed much after MCH immobilized on electrode (curve 3). After the addition of amplification products, the redox current decreased (curve 4), which demonstrated that MB molecules moved away from the electrode surface through the conformation change induced by hybridization. Therefore, the CV results manifested the success of Cp opened by outputs.

EIS is a useful technique for characterizing the step wise modified electrode. The semicircle diameter of EIS equals the electron-transfer resistance (Ret). All EIS data were simulated by Randless circuit showed in the inset of Fig. 2C. As shown in Fig. 2C, the linearity curves represented simulated results and the point curves meant measured results (Zhu et al., 2015a). The

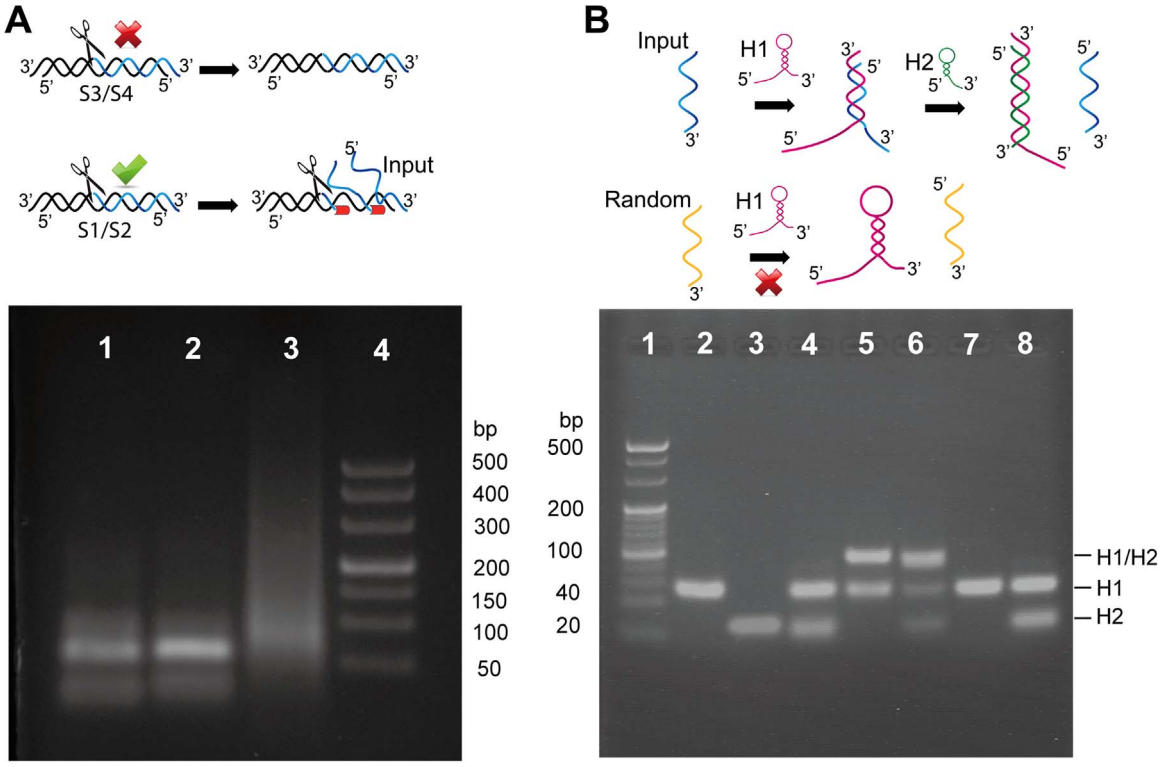

Fig. 1. (A) Gel electrophoresis: (1) Amplification products of S1/S2 without nicking enzyme; (2) Amplification products of S3/S4; (3) Amplification products of S1/S2; (4) DL 500 DNA marker. (B) Gel electrophoresis: (1) 20 bp DNA Ladder; (2) H1; (3) H2; (4) H1 + H2; (5) H1 + Input; (6) H1 + H2 + Input; (7) H1 + Random; (8) H1 + H2 + Random.

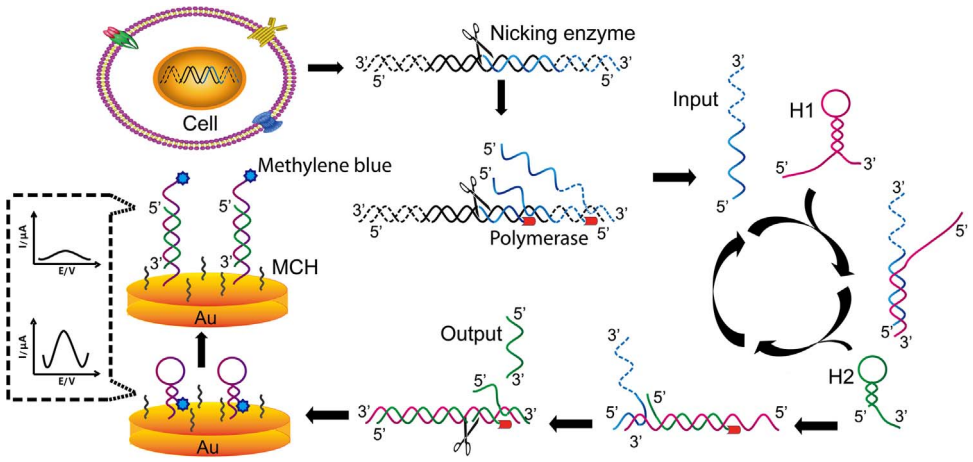

Scheme 1. Schematic illustrating the principle of electrochemical biosensor for Wnt7B gene detection based on enzymatic isothermal amplification.

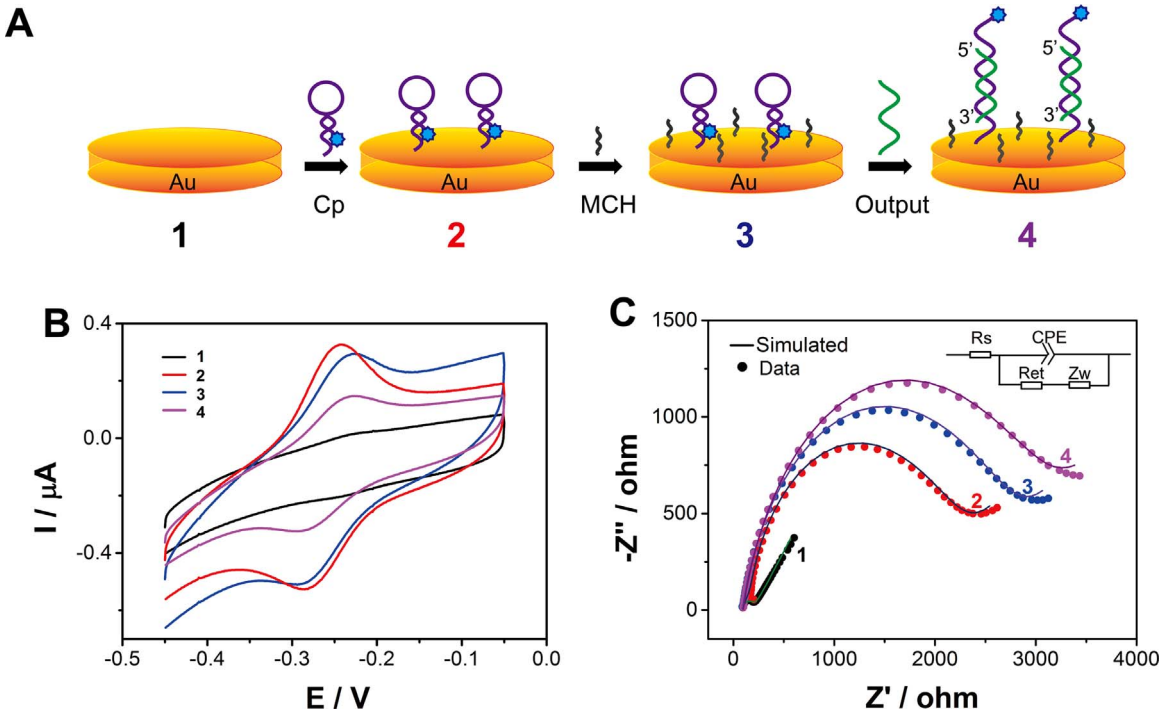

Fig. 2. (A) Each step of the working electrode preparation. (B) CV of: (1) Bare Au electrode; (2) Cp/Au electrode; (3) MCH/Cp/Au electrode; (4) amplification products/MCH/Cp/Au electrode; Buffer**:** 20 mM Tris–HCl, 140 mM NaCl and 5 mM $MgCl_2$ (pH 7.4). (C) EIS of: (1) Bare Au electrode; (2) Cp/Au electrode; (3) MCH/Cp/Au electrode; (4) amplification products/MCH/Cp/Au electrode. linearity curves: simulated results; point curves: measured results. Buffer**:** 0.1 M PBS, 5 mM $[Fe(CN)_6]^{3-/4-}$ and 0.1 M KCl (pH 7.0).

calculation result showed that Ret of the bare Au electrode was very low (curve 1), which demonstrated a good electron transfer ability at the electrode surface. The Ret increased after immobilization of Cp on the electrode surface (curve 2), suggesting that probes were successfully combined on the electrode surface through Au-S bond. A further increase of the semicircle could be found after MCH immobilized on electrode (curve 3). This could be related to the blocking effect of MCH to permeation of electron to the surface of the electrode. After hybridization with amplification products, an increase of Ret was observed (curve 4), implying the output strand hybridized with Cp and added negative charge on the electrode. Therefore, these results confirmed that the immobilization process of each step had been successfully conducted.

3.3. *Feasibility and specificity analysis*

The feasibility of this dsDNA detection method was investigated using SWV method. As shown in Fig. 3A, upon hybridization with the amplification products of single-stranded input, an obvious current signal was observed. For the double-stranded conformation of output with Cp moved a number of MB molecules away from the electrode surface, which suppressed electron transfer. By contrast, a greater decrease in current signal was obtained when the biosensor was incubated with the amplification products of the same concentration of S1/S2. These results indicated that single-stranded input could accurately generate from double-stranded target by nicking enzyme digestion and polymerase polymerization, which could induce greater variation in signal. In addition, the current response only changed slightly

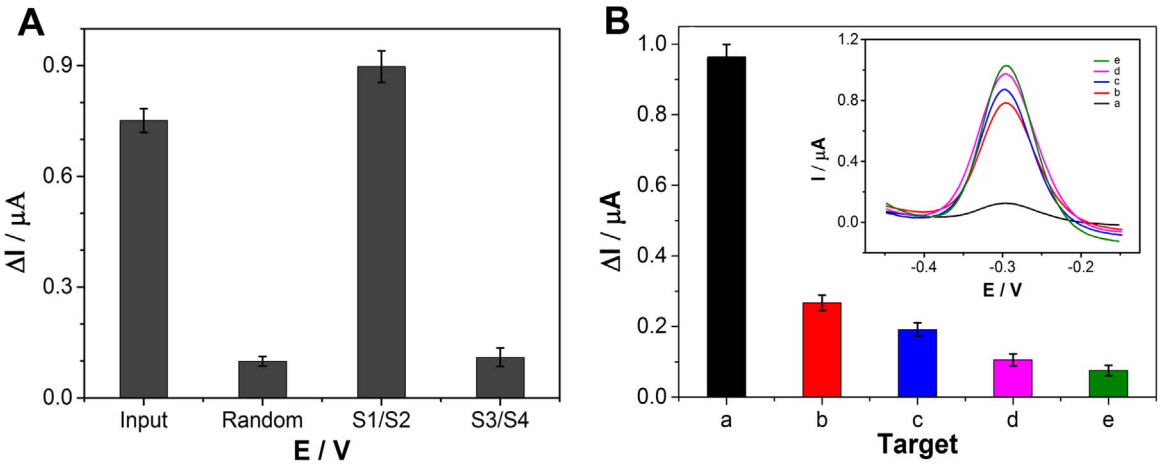

Fig. 3. (A) Feasibility analysis of this method in dsDNA. Current variation of the electrochemical biosensor to amplification products of single-stranded input; single-stranded random DNA; double-stranded target and double-stranded negative control. The DNA concentration was 100 pM. (B) Specificity of the method: (a) complementary input strand; (b) one-base mismatch input; (c) two-base mismatch input; (d) random input DNA; (e) blank. Inset: the SWV curves of different DNA sequences and the blank. The DNA concentration was 5 nM.

upon the addition the amplification products of single-stranded random DNA, which indicated that the amplification reaction could not happen by inaccurate input. Meanwhile, another weak current response of negative control S3/S4 was observed, which suggested that the signal amplification reaction could not proceed without right enzyme nicking site.

To evaluate the specificity of the method, four kinds of input sequences including the complementary input, the single-base mismatch input, the two-base mismatch input and the non-complementary random input were tested (insert in Fig. 3B) under the same experimental conditions. As shown in Fig. 3B, among the four types of DNA sequences, the current variation of complementary strand was much greater than that of the other mismatched sequences. The current variation to single-base mismatched strand was only 33.3% of that to perfectly complementary input, and the signal of perfectly complementary input was 4.1 × that for two-base mismatched sequence. In addition, the signal of random input strand showed an even smaller current variation, and its result was nearly the blank control. Thus, it was believed that the proposed method is strongly selective to target. These results showed that the developed E-DNA sensor with the amplification method could be carried out to accurately detect dsDNA.

3.4. Optimization of the experiment conditions

To reach optimal analytical performance of the electrochemical nucleic acid detection method, the concentration of Cp, the time of Cp immobilization on the electrode, the time of reaction, and the time of output hybridized with Cp were selectively optimized. As shown in Fig. S4, current variation increased with the adding of Cp concentration until 1 μM. Afterward, the current variation was slightly decreased with the further increasing of Cp concentration, indicating a high surface density of Cp could decrease the DNA hybridization efficiency, resulting from steric crowding effects. Thus, it could conclude that the optimal probe concentration was 1 μM, which was used in the following experiments. The effect of probe immobilization time on the signal response was also studied in the range of 2–12 h (Fig. S5). Keeping the other conditions the same, with the immobilization time increase the current variation was enhanced. While, it tended to decrease after 8 h, which indicated that 8 h was the optimal condition.

The time of amplification reaction was an important factor in the sensing system, as background signal could grow with time extension. The current variation of different reaction times in the presence and absence of target were showed in Fig. S6. The black pillars represented the current variation of biosensor incubating with amplification products (in the presence of target) products and the red pillars stood for the current variation of biosensor incubating with amplification products without target. When the reaction time was prolonged, the current variation changed quickly. At the same time, in the absence of target, the current variation (background signal) also increased. Though the current signal in 60 min was higher than other times, its noise was also the highest. Therefore, 40 min was selected as the optimized amplification time due to the maximum signal to noise ratio. To further optimize the analytical performance, the time of output hybridized with probe was investigated. As illustrated in Fig. S7, the current variation increased gradually within 120 min and then reached a platform. Thus, it could conclude that the optimal hybridization time was 120 min

3.5. Analytical performance of the biosensor

Under the optimized conditions, the analytical performance of this method was evaluated by SWV measurements. The current responses upon the target concentrations in the range from 0 fM to 3 nM were shown in Fig. 4A. The addition of target resulted in a signal decrease compared with the blank (curve 1). Fig. 4B illustrates the dependence of the current response upon the target concentrations range from 2 fM to 3 nM. The current response decreased linearly along with the increasing concentration of target DNA from 2 fM to 500 pM (inset in Fig. 4B). The regression equation can be expressed as $\Delta I\ (\mu A) = 2.5605 + 0.1657\ \log C\ (M)$ with a correlation coefficient of 0.9934, where ΔI was the current variation and C was the concentration of target DNA (n = 3). The limit of detection (LOD) at a signal to noise ratio of 3 was calculated to be 1.6 fM. More comparisons of our work with previously reported dsDNA detection methods were shown in Table S1. It could be seen that our developed method could be used to detect dsDNA target simply, sensitively and effectively.

3.6. Reproducibility and stability

The reproducibility of the sensor was investigated at the double-stranded target concentrations of 0.01 pM, 1 pM, and 100 pM. The relative standard deviations (RSD) for six independent measurements were 7.9%, 6.2%, and 4.5% respectively (Fig. S8). Stability

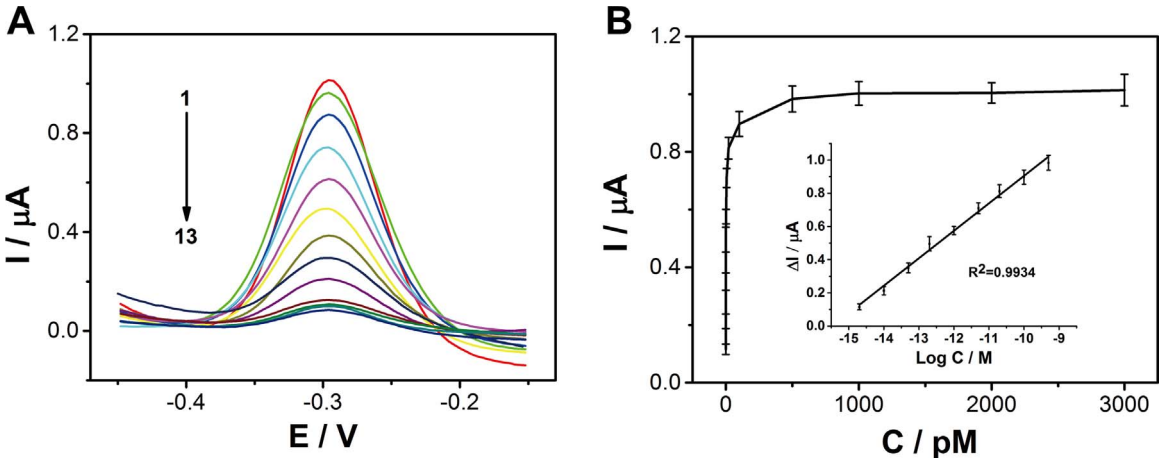

Fig. 4. (A) SWVs of the electrochemical biosensor with the increasing concentrations of target DNA (from 1 to 13: 0, 0.002, 0.01, 0.05, 0.2, 1, 5, 20, 100, 500, 1000, 2000, 3000 pM, respectively). (B) Linear relationship between the current response suppression and target concentration. Inset: calibration curve of the SWV current decrement versus the logarithm of complementary DNA concentration. Error bars represent standard deviations of the measurements (n=3).

of the fabricated biosensor was also examined. The MCH/Cp/Au electrode was stored at 4 °C, and over 94.8% of the initial response retained after a storage period of two weeks. The results demonstrated that the approach possessed satisfactory stability.

3.7. Real sample detection

As shown in Fig. S9, the enzyme cutting portion was a specific DNA fragment and elaborately selected from Wnt7B gene. The enzyme recognition domain in Wnt7B gene is 56152-56156. Furthermore, the target was a relatively conservative sequence through comparing with the gene of mouse (NC_000081.6) by BLAST (Fig. S10). The real sample was extracted from MDA-MB-231 cell, which was the cancer cell about triple negative breast cancer (Sekar et al., 2014; Yeo et al., 2014). Besides, we chose 293T cell as negative control, which was non-carcinous cell coming from human renal epithelial (Wang et al., 2013). PCR was used to prove the gene existence in MDA-MB-231 cells. Primers were designed to amplify a 155 bp section of the Wnt7B gene using NCBI/Primer-BLAST.

The electrophoresis results in our study showed this gene obvious express in MDA-MB-231 cells. Meanwhile, the expression quantity of this gene in 293T cells was low (Fig. 5A). The SWV results showed in the inset of Fig. 5B. The signal of MDA-MB-231 was greater than that of 293T, which was consistent with the results of electrophoresis (as shown in Fig. 5B). The results indicated that this isothermal dsDNA detection method could be used to detect oncogene in real samples simply, specifically and sensitively. Furthermore, the detection time required for this approach was short.

4. Conclusions

In the present study, we have developed a novel and practical electrochemical method to detect Wnt7B gene through isothermal amplification. This method had the following four highlighted advantages: (1) ssDNA produced from dsDNA target using nicking enzyme exploited and polymerase extension. The ssDNA could be detected directly without other complex programs; (2) A low DNA content could be detect due to the isothermal amplification process; (3) Both the specific recognition of nicking enzyme and hairpin self-assembly triggered recycling ensured the high

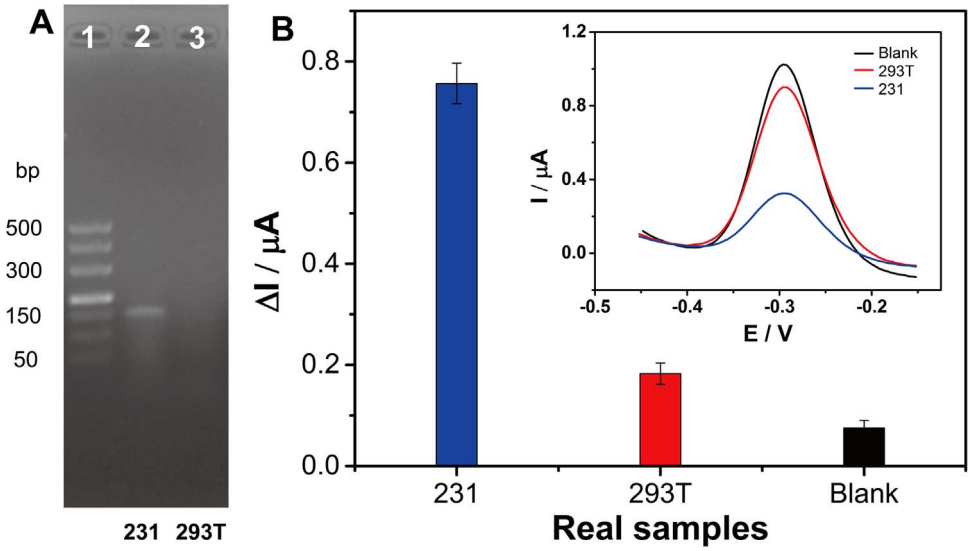

Fig. 5. (A) PCR products of Wnt7B gene from MDA-MB-231 and 293T. Gel electrophoresis: (1) DL500 DNA marker; (2) MDA-MB-231 (155 bp); (3) 293T. (B) Current variation of the electrochemical biosensor to isothermal amplification products of real samples and blank. Inset: SWVs of MDA-MB-231, 293T and blank control, respectively. The DNA concentration was 100 ng/μL.

selectivity of this method; (4) The proposed strategy could be extended to the detection of other DNA by simply exchanging the corresponding DNA sequence. In our study, this method was applied to detect Wnt7B gene in MDA-MB-231 cells with a good analytical performance. In conclusion, the proposed detection method will be a useful platform for oncogene detection, which has great potential in early and rapid diagnosis of cancer.

Acknowledgments

This work was financially supported by National Natural Science Foundation of China (No. 81171415) and Chongqing Medical Scientific Research Projects (20142167).

Appendix A. Supplementary material

Supplementary data associated with this article can be found in the online version at http://dx.doi.org/10.1016/j.bios.2016.06.031.

References

Ali, M.M., Li, F., Zhang, Z., Zhang, K., Kang, D.K., Ankrum, J.A., Le, X.C., Zhao, W., 2014. Chem. Soc. Rev. 43 (10), 3324–3341.
Almario, R.U., Karakas, S.E., 2015. Horm. Metab. Res. 47 (2), 152–157.
Barreda-Garcia, S., Gonzalez-Alvarez, M.J., de-los-Santos-Alvarez, N., Palacios-Gutierrez, J.J., Miranda-Ordieres, A.J., Lobo-Castanon, M.J., 2015. Biosens. Bioelectron. 68, 122–128.
Campuzano, S., Pedrero, M., Garcia, J.L., Garcia, E., Garcia, P., Pingarron, J.M., 2011. Anal. Bioanal. Chem. 399 (7), 2413–2420.
Cai, B., Wang, S., Huang, L., Ning, Y., Zhang, Z., Zhang, G.J., 2014. ACS Nano 8, 2032–2038.
Chen, S.X., Zhang, D.Y., Seelig, G., 2013. Nat. Chem. 5 (9), 782–789.
Fan, C., Plaxco, K.W., Heeger, A.J., 2003. Proc. Natl. Acad. Sci. USA 100 (16), 9134–9137.
Ghindilis, A.L., Smith, M.W., Simon, H.M., Seoudi, I.A., Yazvenko, N.S., Murray, I.A., Fu, X., Smith, K., Jen-Jacobson, L., Xu, S.Y., 2015. Sci. Rep. 5, 7737.
Giljohann, D.A., Mirkin, C.A., 2009. Nature 462 (7272), 461–464.
Hun, X., Xie, G., Luo, X., 2015. Chem. Commun. 51 (33), 7100–7103.
Jia, H., Li, Z., Liu, C., Cheng, Y., 2010. Angew. Chem. 49 (32), 5498–5501.
Jung, C., Ellington, A.D., 2014. Acc. Chem. Res. 47 (6), 1825–1835.
Khodakov, D.A., Khodakova, A.S., Linacre, A., Ellis, A.V., 2013. J. Am. Chem. Soc. 135 (15), 5612–5619.
Li, C., Wang, H., Shen, J., Tang, B., 2015. Anal. Chem. 87 (8), 4283–4291.
Liang, C., Li, D., Zhang, G., Li, H., Shao, N., Liang, Z., Zhang, L., Lu, A., Zhang, G., 2015. Analyst 140 (10), 3439–3444.
Lin, C., Chen, Y., Cai, Z., Luo, F., Wang, Y., Chen, X., 2014. Electrochim. Acta 147, 785–790.
Liu, G., Wan, Y., Gau, V., Zhang, J., Wang, L., Song, S., Fan, C., 2008. J. Am. Chem. Soc. 130, 6820–6825.
Ma, C., Han, D., Deng, M., Wang, J., Shi, C., 2015. Chem. Commun. 51 (3), 553–556.
Ma, C., Li, C., He, N., Wang, F., Ma, N., Zhang, L., Lu, Z., Ali, Z., Xi, Z., Li, X., Liang, G., Liu, H., Deng, Y., Xu, L., Wang, Z., 2012. J. Biomed. Nanotechnol. 8 (6), 1000–1005.
Marimuthu, C., Tang, T.H., Tominaga, J., Tan, S.C., Gopinath, S.C., 2012. Analyst 137 (6), 1307–1315.
Nie, J., Zhao, M.-Z., Xie, W.J., Cai, L.-Y., Zhou, Y.-L., Zhang, X.-X., 2015. Chem. Sci. 6 (2), 1225–1229.
Notomi, T., Okayama, H., Masubuchi, H., Yonekawa, T., Watanabe, K., Amino, N., Hase, T., 2000. Nucleic Acids Res. 28, e63.
Qian, J., Ferguson, T.M., Shinde, D.N., Ramirez-Borrero, A.J., Hintze, A., Adami, C., Niemz, A., 2012. Nucleic Acids Res. 40 (11), e87.
Sekar, T.V., Foygel, K., Ilovich, O., Paulmurugan, R., 2014. Theranostics 4 (5), 460–474.
Shi, C., Liu, Q., Zhou, M., Zhao, H., Yang, T., Ma, C., 2016. Sens. Actuators B Chem. 222, 221–225.
Schweitzer, B., Roberts, S., Grimwade, B., Shao, W., Wang, M., Fu, Q., Shu, Q., Laroche, I., Zhou, Z., Tchernev, V.T., Christiansen, J., Velleca, M., Kingsmore, S.F., 2002. Nat. Biotechnol. 20, 359–365.
Stevenson, R., Baxter, H.C., Aitken, A., Brown, T., Baxter, R.L., 2008. Bioorg. Chem. 36 (5), 215–219.
Van Ness, J., Van Ness, L.K., Galas, D.J., 2003. Proc. Natl. Acad. Sci. USA 100 (8), 4504–4509.
Vincent, M., Xu, Y., Kong, H., 2004. EMBO Rep. 5 (8), 795–800.
Wang, J., Teng, Z., Tian, Y., Fang, T., Ma, J., Sun, J., Zhu, F., Wu, J., Wang, X., Yang, N., Zhou, X., Yun, S., Lu, G., 2013. J. Biomed. Nanotechnol. 9 (11), 1882–1890.
Wang, T., Zhang, Z., Li, Y., Xie, G., 2015. Sens. Actuators B Chem. 221, 148–154.
Wang, Q., Gan, X., Zang, R., Chai, Y., Yuan, Y., Yuan, R., 2016. Biosens. Bioelectron. 81, 382–387.
Wong, J.K., Yip, S.P., Lee, T.M., 2014. Small 10 (8), 1495–1499.
Wu, C., Cansiz, S., Zhang, L., Teng, I.T., Qiu, L., Li, J., Liu, Y., Zhou, C., Hu, R., Zhang, T., Cui, C., Cui, L., Tan, W., 2015. J. Am. Chem. Soc. 137 (15), 4900–4903.
Xu, J., Wu, Z.S., Shen, W., Xu, H., Li, H., Jia, L., 2015. Biosens. Bioelectron. 73, 19–25.
Xuan, F., Hsing, I.M., 2014. J. Am. Chem. Soc. 136 (28), 9810–9813.
Xue, L., Qiu, H., Li, Y., Lu, L., Huang, X., Qu, Y., 2011. Colloid Surf. B 82 (2), 432–437.
Yang, S., Rothman, R.E., 2004. Lancet Infect. Dis. 4 (6), 337–348.
Yeo, E.J., Cassetta, L., Qian, B.Z., Lewkowich, I., Li, J.F., Stefater 3rd, J.A., Smith, A.N., Wiechmann, L.S., Wang, Y., Pollard, J.W., Lang, R.A., 2014. Cancer Res. 74 (11), 2962–2973.
Yin, P., Choi, H.M., Calvert, C.R., Pierce, N.A., 2008. Nature 451 (7176), 318–322.
Zang, Y., Lei, J., Hao, Q., Ju, H., 2016. Biosens. Bioelectron. 77, 557–564.
Zhu, B., Alsager, O.A., Kumar, S., Hodgkiss, J.M., Travas-Sejdic, J., 2015a. Biosens. Bioelectron. 70, 398–403.
Zhu, J., Zhang, L., Dong, S., Wang, E., 2015b. Chem. Sci. 6, 4822–4827.